JB Journals.ASM.org

The DNA-Binding Protein from Starved Cells (Dps) Utilizes Dual Functions To Defend Cells against Multiple Stresses

Vlad O. Karas,* Ilja Westerlaken, Anne S. Meyer

Department of Bionanoscience, Kavli Institute of Nanoscience, Delft University of Technology, Delft, Netherlands

ABSTRACT

Bacteria deficient in the DNA-binding protein from starved cells (Dps) are viable under controlled conditions but show dramatically increased mortality rates when exposed to any of a wide range of stresses, including starvation, oxidative stress, metal toxicity, or thermal stress. It remains unclear whether the protective action of Dps against specific stresses derives from its DNA-binding activity, which may exclude destructive agents from the chromosomal region, or its ferroxidase activity, which neutralizes and sequesters potentially damaging chemical species. To resolve this question, we have identified the critical residues of *Escherichia coli* Dps that bind to DNA and modulate iron oxidation. We uncoupled the biochemical activities of Dps, creating Dps variants and mutant *E. coli* strains that are defective in either DNA-binding or ferroxidase activity. Quantification of the contribution of each activity to the protection of DNA integrity and cellular viability revealed that both activities of Dps are required in order to counteract many differing stresses. These findings demonstrate that Dps plays a multipurpose role in stress protection via its dual activities, explaining how Dps can be of vital importance to bacterial viability over a wide range of stresses.

IMPORTANCE

The DNA-binding protein from starved cells (Dps) protects bacterial cells against many different types of stressors. We find that DNA binding and iron oxidation by Dps are performed completely independently of each other. Both biochemical activities are required to protect *E. coli* against stressors, as well as to protect DNA from oxidative damage *in vitro*. These results suggest that many stressors may cause both oxidative stress and direct DNA damage.

The ability to adapt to changes in the environment is one of the key determinants of the fitness of a species. Bacteria have evolved a multitude of ways to survive and prosper under stressful conditions, ranging from extreme measures such as sporulation to the expression of specialized stress mediation proteins (1–3). One such protein vital in stress survival is the DNA-binding protein from starved cells (Dps) (4), which is conserved to a remarkable degree in more than 300 bacterial species (5). In *Escherichia coli*, Dps acts as a component of several stress response pathways; it can be independently upregulated as a member of the OxyR regulon in exponentially growing cells or via σ^S in stationary-phase cells (6). The presence of Dps enhances bacterial survival of many different stresses, including starvation, heat shock, oxidative stress, and overexposure to iron (7, 8). These protective effects of Dps expression are presumably due to one or both of its dual biochemical functions, DNA binding and ferroxidase activity (9), but the molecular mechanisms and physiological consequences of these activities are not yet fully elucidated.

E. coli Dps binds to DNA *in vitro* with no apparent sequence specificity, forming a highly stable complex (7, 10). Dps is a minor component of the *E. coli* nucleoid during exponential phase, but its concentration rises dramatically during stationary phase until Dps becomes the predominant nucleoid-associated protein (11). Extended periods of interaction between Dps and DNA, both *in vivo* and *in vitro*, can result in Dps compacting the DNA into a highly ordered crystalline structure (12, 13). This striking DNA-binding behavior has been challenging to explain biochemically. Crystallographic studies have shown that *E. coli* Dps assembles into a spherical, 12-membered homo-oligomer with a hollow core (14). The outer surface of the Dps oligomer does not display any known DNA-binding motifs and is mostly negatively charged and thereby potentially repulsive to a similarly charged DNA molecule (14). Not resolved in the *E. coli* Dps crystal structure were the disordered N-terminal regions of each Dps monomer, which extend outward from the dodecamer and contain several lysines, proposed to contribute to DNA binding (14) (Fig. 1A). Removal of large sections of the N-terminal region reduce DNA condensation by Dps (15), but the exact molecular interactions that cause DNA binding remain unclear.

Dps family members contain a highly conserved ferroxidase center located at their dimeric interfaces (4). These residues catalyze the oxidation of Fe(II) ions by hydrogen peroxide to produce Fe(III), which is mineralized and stored within the Dps cavity (16, 17). Each ferroxidase center in *E. coli* Dps contains two iron-bind-

Received 11 June 2015 **Accepted** 22 July 2015

Accepted manuscript posted online 27 July 2015

Citation Karas VO, Westerlaken I, Meyer AS. 2015. The DNA-binding protein from starved cells (Dps) utilizes dual functions to defend cells against multiple stresses. J Bacteriol 197:3206–3215. doi:10.1128/JB.00475-15.

Editor: R. L. Gourse

Address correspondence to Anne S. Meyer, a.s.meyer@tudelft.nl.

* Present address: Vlad O. Karas, Institute of Molecular Life Sciences, University of Zurich, Zürich, Switzerland.

V.O.K. and I.W. contributed equally to this work.

Supplemental material for this article may be found at http://dx.doi.org/10.1128/JB.00475-15.

doi:10.1128/JB.00475-15

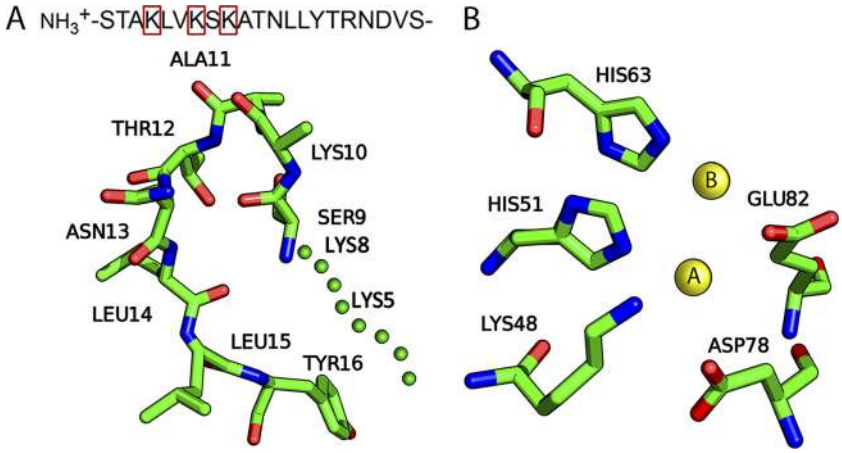

FIG 1 Dps active-site structures. (A) The N-terminal region of Dps, as determined by Grant et al. (14). Residues that were altered in this study are boxed (top). The first amino acid of the Dps protein is Ser2, because of posttranslational cleavage of the N-terminal methionine (48, 49). (B) The ferroxidase active site, with predicted iron atoms indicated as yellow spheres (14, 16, 17).

ing sites with differing affinities (16). The stronger A site is coordinated by the His51, Glu82, and Asp78 residues. The weaker B site is coordinated by His63 and Glu82 and frequently contains a water molecule unless Dps is saturated with iron (16, 17) (Fig. 1B). The weak affinity of the B site is speculated to be due to a salt bridge between the Lys48 and Asp78 residues (16). Despite the extensive crystallographic investigation of the Dps ferroxidase center, the contribution of specific residues to Dps ferroxidase activity has yet to be determined biochemically.

In this study, we have unraveled the role of each Dps activity in *E. coli* stress protection by selectively modifying Dps activities. Targeted residue substitutions in the Dps N-terminal region and ferroxidase center created Dps point variants with either modified DNA binding affinity or ferroxidase activity, while leaving the other function unaffected. These experiments identified critical DNA-binding lysine residues and also pinpointed the crucial residues involved in Dps iron oxidation. An *in vitro* DNA protection assay showed that alteration of the strength of either biochemical activity correlated with the ability of each Dps variant to protect DNA from oxidative degradation. We also quantified the contributions of Dps ferroxidase activity and DNA binding to bacterial survival under stress with *in vivo* viability assays, revealing that both activities are required for Dps protection under a wide variety of different stress conditions. Thus, this work reveals that the DNA-binding and ferroxidase activities of Dps are biochemically separable but function jointly to preserve DNA integrity and cellular viability.

MATERIALS AND METHODS

Site-directed mutagenesis. Site-directed mutagenesis was performed according to the QuikChange protocol (Stratagene). Codons with the highest coding frequencies were chosen for substitutions in the *dps* gene. The sequences of the forward primers used are as follows, with altered base pairs underlined: K5A, 5′-CATATGAGTACCGCTGCGTTAGTTAAATCAAAAGC-3′; K8A, 5′-GTACCGCTAAATTAGTTGCGTCAAAAGCGACCAATC-3′; K10A, 5′-GCTAAATTAGTTAAATCAGCGGCGACCAATCTGCTTTATACC-3′; K48H, 5′-CTTTCTTTGATTACCCATCAAGCGCACTGGAAC-3′; H51A, 5′-GATTACCAAACAAGCGGCCTGGAACATGCGCGGCGCT-3′; D78A, 5′-CTGATCGATCATCTGGCGACCATGGCAGAACG-3′.

PCR was performed with Phusion polymerase (Promega) by using a pET-17b-dps plasmid (18) as the template. The PCR product was digested with DpnI and used to transfect chemically competent *E. coli* TOP10 cells. Successful mutagenesis was confirmed by sequencing.

Dps purification. Dps purification was performed as described by Karas et al. (18). Briefly, a pET-17b plasmid containing Dps was transfected into *E. coli* BL21(DE3)pLysS. Cells were grown at 37°C with shaking at 250 rpm to an optical density at 600 nm (OD_{600}) of 0.4 to 0.6. Dps expression was induced with isopropyl-β-D-thiogalactopyranoside (IPTG) for 4 h. The cells were disrupted with a French press. After clarification, the lysate was purified with a combination of ion-exchange column chromatography (DEAE-Sepharose and SP Sepharose; GE Healthcare) and ammonium sulfate precipitation. The concentration of purified Dps samples was determined by measuring the absorbance at 280 nm, with a molar extinction coefficient of 15,470 M^{-1} cm^{-1} for the Dps monomer. The oligomeric stoichiometries of purified wild-type Dps and all Dps point variants were determined via gel filtration on a Superdex 200 Increase 10/300 GL column (GE Healthcare).

DNA binding assay. Linear DNA (331 bp, 2.5 nM final concentration) and Dps (final monomer concentration of 0.075 to 5 μM for wild-type Dps and H51A, K48A, and D78A mutant Dps; 2.5 to 50 μM for K5A mutant Dps; or 5 to 150 μM for K8A and K10A mutant Dps) was added to 1× PDB buffer (25 mM HEPES-KOH [pH 7.6], 5 mM $MgCl_2$, 5 mM KCl, 0.032% NP-40, 10% glycerol). Ingredients were mixed and incubated for 30 min at 30°C. Samples were put on ice, mixed with DNA loading dye (6× Blue/Orange Loading Dye; Promega), and loaded onto an unstained gel (0.6% agarose in 0.5× TB buffer, prerun for 30 min at 80 V and 4°C). Electrophoresis was performed at 4°C for 2 to 3 h at 80 V. The gel was poststained with Sybr Gold dye (Invitrogen) for 30 min at 4°C. Imaging was performed on a Typhoon scanner (GE Healthcare) with an excitation wavelength (λ_{ex}) of 488 nm, an emission wavelength (λ_{em}) of 520 nm, a photomultiplier tube (PMT) voltage of 300 to 400 V, and a 50-μm pixel size. ImageQuant software was used for band intensity quantification. The fraction of bound DNA was calculated as 100% minus the fraction of unbound DNA, based on a no-DNA control lane. The data were fitted to the Hill equation ($\theta = L^n/[K_D + L^n]$) with OriginPro to determine the apparent K_D and n parameters of binding. All fits had an R^2 value of 0.98 or higher. Each reaction was performed at least in triplicate. All errors are expressed as the standard error of the mean.

Ferroxidase assay. The following solutions were prepared fresh under a nitrogen atmosphere and kept in airtight vials to reduce oxygen contamination during measurements: 1 mM $FeSO_4$, 500 μM H_2O_2 (shielded from light and on ice), and 1× reaction buffer (100 mM morpholinepropanesulfonic acid [MOPS]-KOH [pH 7], 100 mM NaCl). Dps (final do-

decamer concentration, 0.5 μM for N-terminal mutant proteins and 2 μM for ferroxidase center mutant proteins) was added to 1× reaction buffer to a total volume of 100 μl, and this sample was used to blank the spectrophotometer (NanoDrop 2000c). For ferroxidase activity measurements, Dps was mixed with 1× reaction buffer, and then $FeSO_4$ was added (final concentration range, 3 to 72 μM), mixed, and allowed to incubate for 30 s. Hydrogen peroxide was added to a concentration equal to 0.5 times the [$FeSO_4$] (1.5 to 36 μM) in a final volume of 100 μl and mixed with a pipette. The cuvette was rapidly inserted into the spectrophotometer, and a kinetic measurement program was initiated (measurement of absorbance at 304 nm at 3-s intervals for a total of 800 s). The output file was exported into OriginPro, in which the initial slope (typical interval: $t = 10$ to 40 s) of the oxidation curve was fitted linearly. Each reaction was performed at least in triplicate. All errors are expressed as the standard error of the mean.

DNA protection assay. $FeSO_4$ at 2 mM was freshly prepared under a nitrogen atmosphere and stored in an airtight vial. A stock solution of 100 mM H_2O_2 was freshly made and kept in the dark on ice. Linear DNA (2.8 kb; linearized plasmid pUC19) was diluted in 12× reaction buffer (1 M MOPS-KOH [pH 7], 1 M NaCl) to a concentration of 100 ng/μl, and 1 μl of the mixture was added to a reaction tube. Water was added to bring the final volume to 12 μl (without SDS), and then 3 μM dodecamer Dps was added. In the case of the bovine serum albumin (BSA) control conditions, 3 μM BSA was added in place of Dps. The mixture was incubated for 15 min at room temperature to allow Dps-DNA binding to occur. $FeSO_4$ solution was added (final concentration of 0 to 1 mM), quickly followed by hydrogen peroxide (final concentration of 10 mM). The reaction mixture was mixed and allowed to incubate for 5 min at room temperature. A 0.8-μl volume of 20% SDS was added, mixed, and incubated at 85°C to dissociate the DNA-Dps complexes; this was followed by 1 min of incubation on ice. The reaction product was mixed with DNA loading dye (6× Blue/Orange Loading Dye; Promega), run on a 1% agarose gel, and post-stained with ethidium bromide. Imaging was performed on a Typhoon scanner (GE Healthcare) with a λ_{ex} of 532 nm, a λ_{em} of 610 nm, a PMT voltage of 300 to 400 V, and a 50-μm pixel size. ImageQuant software was used for band intensity quantification.

The protocol was modified for the N-terminal Dps variants to better highlight the differences in DNA binding affinity. The incubation step following hydrogen peroxide addition was extended to 1 h. Prior to disaggregation with SDS, the reaction was stopped by adding 1 μl of 0.5 M EDTA and approximately 0.05 g of MnO_2 crystals. The mixture was vortexed for 1 min to allow iron chelation to EDTA and MnO_2-mediated hydrogen peroxide degradation to occur. Each reaction was performed at least in triplicate. All errors are expressed as the standard error of the mean.

Strain construction. All new bacterial strains were created from *E. coli* K-12 strain W3110 (CGSC no. 4474). The *dps* mutant strain was created by replacing the genomic *dps* gene with a counterselectable *cat-sacB* cassette. Lambda red helper plasmid pKD46 (19) was transformed into *E. coli* W3110. The strain was grown in LB medium (50 μg/ml ampicillin, 30°C, 250 rpm) to mid-exponential phase; this was followed by the addition of L-arabinose (final concentration, 0.4%) to induce the expression of the lambda red proteins. After an additional incubation for 1 h at 37°C while shaking, cells were made electrocompetent. Plasmid pKD3V (20) was used as the template for PCR to obtain the counterselectable *cat-sacB* fragment. The primers were decorated with 50-bp homology flanks for recombination (underlined), flanking the *dps* gene in the chromosome, as follows: forward, 5′-TACTTAATCTCGTTAATTACTGGGACATAACATCAAGAGGATATGAAATTTGTAGGCTGGAGCTGCTTCG-3′; reverse, 5′-AGGAAGCCGCTTTTATCGGGTACTAAAGTTCTGCACCATCAGCGATGGATCATATGAATATCCTCCTTAG-3′.

The PCR product was DpnI digested, purified, and transfected into electrocompetent *E. coli* W3110 cells with expressed lambda proteins. Following 4 h of recovery in LB medium, the cells were plated on LB agar containing chloramphenicol at 25 μg/ml. The *dps* knockout was confirmed by colony PCR and sequencing. The newly constructed strain (*E. coli* W3110 *dps*::*cat-sacB*) was grown at 37°C to remove the pKD46 plasmid.

The *dps* knockout strain was used as the template for the creation of Dps mutant strains. The strain was made ready for lambda red recombination and transfected with the mutated *dps* variants flanked by 50-bp chromosomal flanks (underlined, obtained by PCR from pET17b vectors) produced with the following primers: forward for all except for K5A mutant Dps, 5′-TACTTAATCTCGTTAATTACTGGGACATAACATCAAGAGGATATGAAATTATGAGTACCGCTAAATTAG-3′; forward for K5A mutant Dps, 5′-TACTTAATCTCGTTAATTACTGGGACATAACATCAAGAGGATATGAAATTATGAGTACGCTGCGTTAG-3′; reverse for all, 5′-AGGAAGCCGCTTTTATCGGGTACTAAAGTTCTGCACCATCAGCGATGGATTTATTCGATGTTAGACTC-3′.

Homologous recombination was allowed to occur, and cells were plated on NaCl-free LB agar with 10% sucrose (counterselective for *sacB*). Plates were incubated overnight at 30°C. Healthy-looking colonies were restreaked onto LB agar containing chloramphenicol at 25 μg/ml. Colonies that did not grow on chloramphenicol were selected for colony PCR, and gene replacement was verified by sequence analysis.

To ensure clean genetic backgrounds, phage transduction was carried out. Phage P1 lysate was made with the *dps* knockout (donor) strain. An overnight culture of the *dps* knockout strain in LB containing chloramphenicol at 25 μg/ml was diluted 1:50 in LB supplemented with 30 mM $MgSO_4$ and 15 mM $CaCl_2$. The culture was incubated at 37°C for 30 min while shaking. Phage P1 lysate was added to the culture (20 μl of phage/10 ml) and incubated at 37°C for approximately 3 h until the culture became clear. Chloroform was added (200 μl of chloroform/10 ml); this was followed by filtration with a 0.45-μm filter. An overnight culture of wild-type W3110 was diluted 1:10 in LB supplemented with 30 mM $MgSO_4$ and 15 mM $CaCl_2$. Tubes with 1 ml of diluted culture were incubated with dilutions of fresh P1 lysate for 30 min at 37°C while shaking. Cells were pelleted for 3 min at a relative centrifugal force of 10,000, resuspended in LB supplemented with 20 mM Na-citrate, and incubated for 1 h at 37°C while shaking to stop transduction. The cells were pelleted, resuspended in 100 μl of LB with 20 mM Na-citrate, and plated on LB agar with 20 mM Na-citrate and chloramphenicol at 25 μg/ml. Transformants were restreaked several times onto selective plates with 20 mM Na-citrate to prevent readsorption of the phage. Selected transformants were checked by sequence analysis. Western blotting indicated that the Dps expression levels in all of the strains were approximately equivalent.

***In vivo* stress survival assays.** Single colonies of wild-type, *dps* knockout, and *dps* mutant strains were cultured overnight in HiDef Azure medium (Teknova) supplemented with 0.2% glucose at 37°C while shaking. Overnight cultures were diluted in fresh medium to an OD_{600} of 0.04 and grown to mid-exponential phase and an approximate OD_{600} of 0.6. The following stress conditions were applied, at 37°C with shaking unless otherwise indicated: none, 24 h of growth, heat shock (50°C for 30 min), oxidative stress (10 mM H_2O_2 for 15 min), antibiotic stress (spectinomycin at 1 mg/ml for 24 h), iron toxicity (10 mM $FeSO_4$ for 15 min), osmotic shock (500 mM NaCl for 24 h, added to 24-h-old cultures), and 48 h of growth. Samples of stressed cultures were taken and serially diluted in 0.9% NaCl (10^{-1} to 10^{-8}). A 5-μl volume of each dilution was plated in duplicate on LB agar for counting of CFU. Each reaction was performed at least in triplicate. All errors are expressed as the standard error of the mean.

RESULTS

DNA binding by Dps requires N-terminal lysines. The N-terminal region of Dps has been shown to be crucial for DNA binding (15), but the specific amino acids that interact with DNA have not yet been identified. The three lysine residues (K5, K8, and K10) in the disordered N-terminal Dps tail seemed to be likely candidates for binding to DNA because of their opposing electrostatic charges (15). These three lysine residues were individually re-

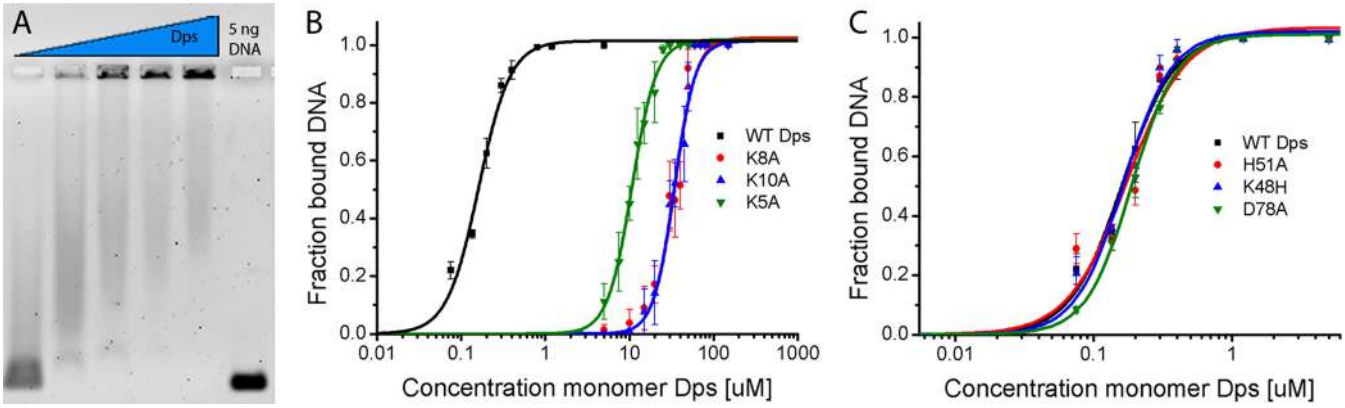

FIG 2 Dps binds DNA through lysines in its N-terminal region. (A) Gel shift assay indicating the amounts of DNA bound to Dps at various Dps concentrations. The amount of bound DNA was monitored by measuring the disappearance of the fluorescent signal at the position on the agarose gel corresponding to unbound DNA. (B, C) DNA-binding curves of N-terminal Dps variants (B) and ferroxidase active-site Dps variants (C) at various Dps concentrations, fitted to the Hill equation ($\theta = L^n/[K_D + L^n]$). WT, wild-type. Reaction mixtures contained wild-type Dps or variants (0.075 to 150 μM monomer) and linear DNA (331 bp, 2.5 nM).

placed with alanine through site-directed mutagenesis, creating the K5A, K8A, and K10A variants of Dps (Fig. 1A). These modified proteins were purified biochemically, and the fraction of assembled dodecameric Dps was determined by gel filtration to be >99.9% for each variant (see Fig. S1 in the supplemental material). The effects of the N-terminal point substitutions on the DNA-binding and iron oxidation properties of Dps were measured *in vitro*.

The DNA-binding affinities of Dps N-terminal variants were tested in a gel shift assay in which purified Dps at various concentrations was incubated with short linear DNA at pH 7.6; this was followed by electrophoresis to detect Dps-dependent complex formation (Fig. 2A). Dps dodecamers form extensive aggregates with DNA *in vitro* within seconds, such that Dps-bound DNA is shifted to the wells of the gel, even when short DNA fragments of <100 bp are used (7, 13, 15). Wild-type Dps was seen to bind DNA in a highly cooperative manner, with a Hill coefficient of 2.9 ± 0.3 and an apparent K_D of 0.165 μM ± 0.007 (Fig. 2B; Table 1). The N-terminal mutant forms of Dps all bound DNA with severely weakened affinity compared to that of wild-type Dps but similar degrees of cooperativity. K5A mutant Dps bound DNA with a 65-fold weaker K_D than wild-type Dps, and K8A and K10A mutant Dps each bound with a 200-fold weaker K_D (Fig. 2B; Table 1). These dramatically weakened affinities indicate that the N-terminal lysine residues play a crucial role in Dps binding to DNA. The variation in affinities among the variants demonstrates that not all of the lysines in the N terminus contribute equally to DNA binding (Fig. 2B; Table 1).

TABLE 1 Biochemical properties of Dps variants[a]

Dps variant	Mean apparent K_D (μM) ± SEM	Mean *n* parameter ± SEM	r_{ferr}
WT	0.165 ± 0.007	2.9 ± 0.3	=
K5A	10.7 ± 0.26	3.0 ± 0.2	=
K8A	34.7 ± 1.8	3.4 ± 0.6	=
K10A	34.1 ± 1.2	3.5 ± 0.4	=
K48H	0.164 ± 0.004	3.0 ± 0.3	+
H51A	0.157 ± 0.02	2.7 ± 0.5	=
D78A	0.178 ± 0.01	3.0 ± 0.2	−

[a] Indicated are the measured apparent K_D and *n* parameter of DNA binding and the strength of ferroxidase activity relative to that of wild-type Dps (=, similar to wild type; +, stronger than wild type; −, weaker than wild-type).

Any effects of the N-terminal mutations on Dps ferroxidase activity were assayed by measuring iron oxidation rates in the presence of Dps and hydrogen peroxide under anaerobic conditions. Iron oxidation rates were measured by determining the initial rate of increase in absorbance at 304 nm caused by the transition of Fe^{2+} to Fe^{3+} (21). In the absence of Dps, the rate of spontaneous iron oxidation was low (Fig. 3B). The iron oxidation rates increased with the iron concentration for each Dps variant, and no significant differences between the rates of wild-type Dps and the N-terminal lysine-to-alanine Dps variants were seen (Fig. 3B). These results indicate that Dps ferroxidase activity was not altered by point mutations that radically weakened DNA-binding affinity.

Dps ferroxidase and DNA-binding activities are fully separable. While the ferroxidase active site of Dps proteins is highly conserved (5), it remains unclear which specific amino acids are functionally required for iron oxidation. Using site-directed mutagenesis, we individually altered two of the coordinating residues for the strong iron-binding site to create H51A mutant Dps and D78A, two variants with potentially weakened ferroxidase activity. We also attempted to create a Dps variant with stronger ferroxidase activity through a K48H mutation, mimicking the ferroxidase center of *Listeria innocua* Dps, which binds iron with higher affinity (16, 22) (Fig. 1B). These Dps variants were purified biochemically, and the fraction of assembled dodecameric Dps of each variant was determined to be >99.9% (see Fig. S1 in the supplemental material). Their iron oxidation and DNA-binding properties were determined *in vitro*.

An intrinsic fluorescence quenching assay revealed that wild-type Dps and the Dps variants each bound to iron with indistinguishable stoichiometries, showing that the ferroxidase site mutations had no effect on that property (data not shown) (17, 22). The effects of the Dps ferroxidase site mutations on iron oxidation rates were then determined (Fig. 3A). Each Dps variant catalyzed iron oxidation at an increasing rate as the iron concentration was increased. As predicted, D78A mutant Dps oxidized iron at a

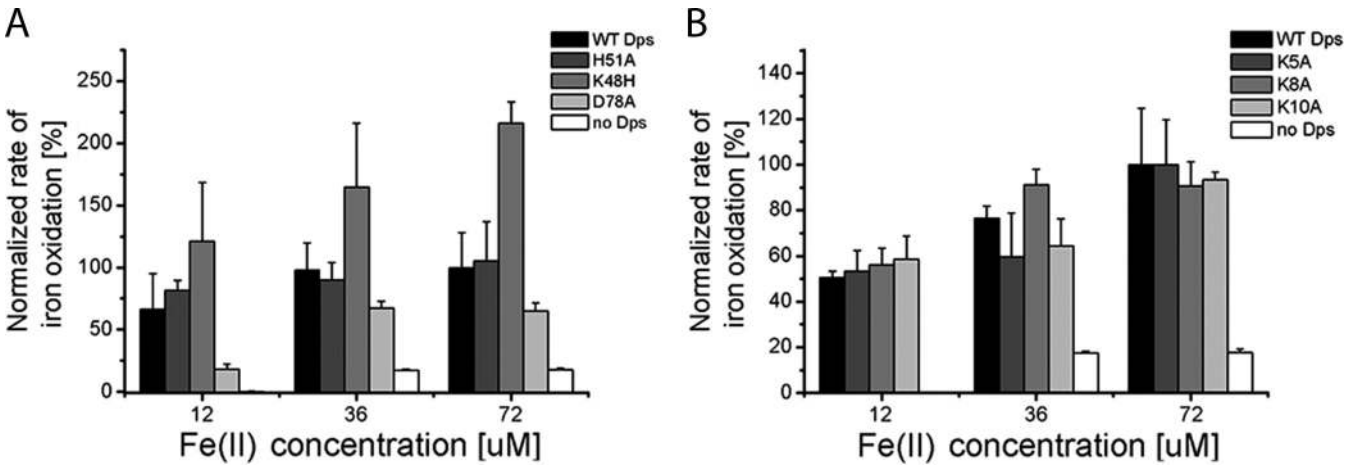

FIG 3 Dps ferroxidase active-site residues contribute unequally to iron oxidation. Rates of iron oxidation were determined by the initial rate of increase in absorbance at 304 nm. Relative ferroxidase activities of ferroxidase active-site variant Dps (A) and N-terminal variant Dps (B) at various iron concentrations are displayed. Iron oxidation rates are normalized against the rate of wild-type (WT) Dps in the presence of 72 μM Fe(II) in each graph.

lower rate than wild-type Dps at every iron concentration tested. However, the H51A substitution did not have the predicted effect; the oxidation rate of this Dps variant was always similar to that of wild-type Dps. These results suggest that Asp78 plays a crucial role in Dps iron oxidation, while His51 is not required. Finally, K48H mutant Dps, the variant designed to have increased ferroxidase activity, oxidized iron faster than wild-type Dps under every condition. This result indicates that altering the Lys48 residue may have indeed created a Dps variant with stronger iron binding at the weak B site, thus strengthening its ferroxidase activity.

The DNA-binding properties of the ferroxidase center mutant Dps proteins were analyzed to determine whether the alterations in ferroxidase activity had affected DNA binding as well. Each of the ferroxidase site mutant (H51A, K48H, and D78A) Dps proteins had DNA-binding affinities and Hill coefficients nearly identical to those of wild-type Dps (Fig. 2C; Table 1). The DNA-binding and ferroxidase activities of Dps are thus completely separable, since each may be altered without changing the other. Furthermore, our experiments confirm the creation of Dps variants that are each altered in only one of their two primary biochemical activities. These variants can be used to test the contribution of each activity to Dps-mediated cellular protection separately.

Both Dps activities are required for *in vitro* DNA protection. One central aspect of Dps stress mediation is the protection of DNA from oxidative damage, which has been documented both *in vivo* and *in vitro* (15, 17, 23, 24). Despite the importance of Dps in DNA protection, it is unclear which Dps activities contribute to the effect: ferroxidase activity, DNA binding, or both? An *in vitro* DNA protection assay was performed to answer this question. The combination of hydrogen peroxide and iron in solution produces damaging hydroxyl radicals through iron-catalyzed degradation of hydrogen peroxide. These radicals cause DNA strand breaks, which can be visualized by electrophoresis (18, 25). The protective effect of Dps under these conditions was quantified by measuring the intensity of the undamaged DNA band at differing concentrations of Fe(II) (Fig. 4A). Wild-type Dps provides dramatic protection of the DNA compared to conditions with no added protein (Fig. 4). An assay performed with added BSA protein showed no additional DNA protection compared to the no-protein condition (Fig. 4B and C), indicating that Dps protection of DNA is specific.

The DNA protection assay was performed in the presence of the N-terminal Dps variants (Fig. 4B) and the ferroxidase center Dps variants (Fig. 4C). The two sets of experiments were performed with slightly altered protocols in order to highlight the differences in protection within each group of Dps variants. Assays of the three N-terminal Dps variants revealed that they all protected DNA less efficiently than wild-type Dps did, with K5A mutant Dps preserving DNA less efficiently than K8A and K10A mutant Dps (Fig. 4B). These results indicate that DNA binding is required for DNA protection by Dps, although the strength of DNA binding did not directly correlate with the strength of DNA protection. Among the ferroxidase center variants, D78A mutant Dps protected DNA less efficiently than did wild-type Dps, H51A mutant Dps had DNA protection capability similar to that of wild-type Dps, and K48H mutant Dps protected DNA more efficiently than did wild-type Dps (Fig. 4C). The relative strength of DNA protection of each Dps variant correlates well with its relative ferroxidase activity, demonstrating that ferroxidase activity also contributes directly to DNA protection.

Bacterial survival of stress benefits from both Dps activities. We next tested the effects of modifying individual Dps activities on bacterial viability under different stress conditions *in vivo*. By two-step lambda red recombination (20), bacterial strains were constructed that carry the characterized Dps active-site point mutations or have *dps* knocked out in a wild-type *E. coli* strain W3110 background (see Fig. S2 in the supplemental material). Two Dps variants were not considered further, i.e., H51A mutant Dps because it behaved identically to wild-type Dps in all *in vitro* assays and Dps K8A because it displayed the same biochemical properties as Dps K10A. The strains of interest were grown in rich defined medium and then subjected to stress (starvation, heat shock, oxidative stress, antibiotic stress, iron toxicity, or osmotic stress); this was followed by determination of the concentration of viable cells. Most stresses were applied to cells in the mid-exponential growth phase, despite the relatively low concentration of Dps protein in exponential-phase cells; otherwise the cells would experience nutritive stress in addition to the stress being assayed, complicating the interpretation of the experiment.

The viability of bacteria with altered Dps activity was indistinguishable from that of the wild-type strain, both in the mid-expo-

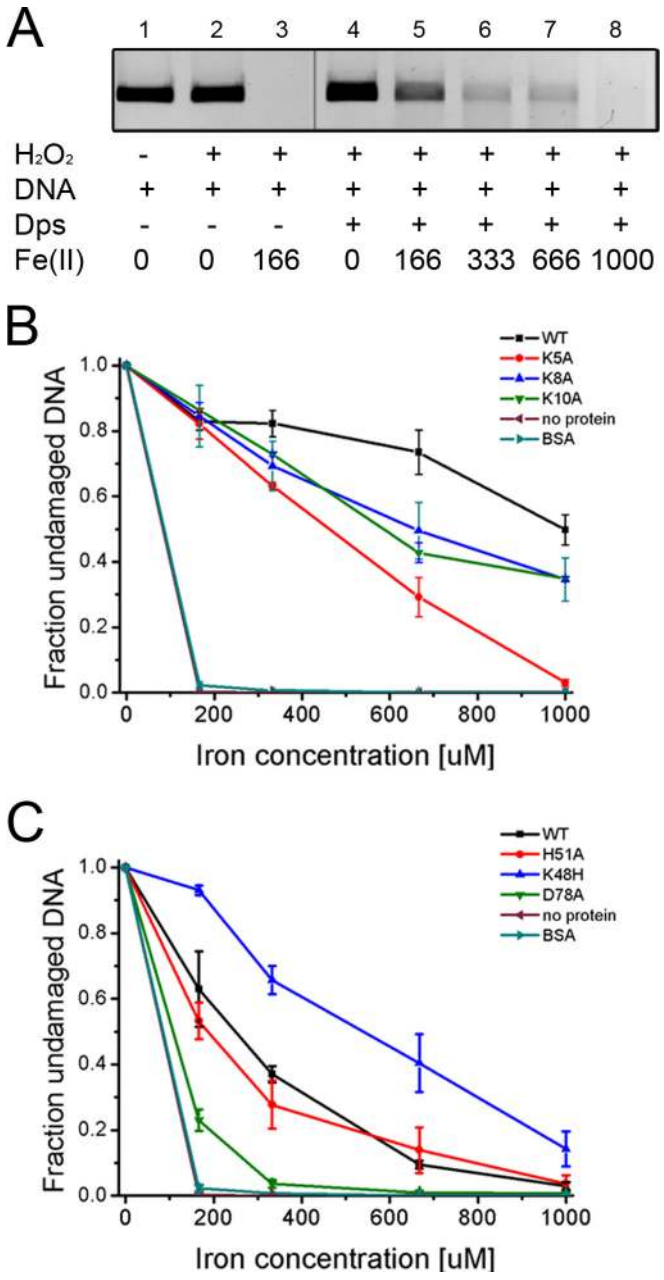

FIG 4 Both Dps activities protect DNA from oxidative degradation. (A) *In vitro* DNA protection assay indicating DNA degradation by reactive oxygen species. DNA degradation was monitored by measuring the disappearance of the fluorescent signal at the position on the agarose gel corresponding to full-length DNA. Micromolar Fe(II) concentrations are indicated. (B, C) DNA protection by N-terminal variants (B) and ferroxidase active-site variants (C) of Dps at various iron concentrations. WT, wild type. The values for the no-protein and BSA control conditions are overlaid upon each other.

nential phase and after 24 h of growth (Fig. 5A and B). In contrast, every other stress condition tested resulted in lower viability of the *dps* knockout strain, as well as the dps^{K5A}, dps^{K10A}, and dps^{D78A} mutants, which display lower DNA-binding or ferroxidase activity than the wild-type strain (Fig. 5C to H). The dps^{K48H} mutant, which exhibits increased ferroxidase activity, was similar in viability to wild-type *E. coli* under these stress conditions (Fig. 5C to H). Both DNA-binding and ferroxidase activities are therefore required for Dps to protect bacterial viability during stress, for a broad range of different types of stressors.

DISCUSSION

Dps plays a multifaceted role in bacterial stress mediation. *E. coli* Dps has two major distinct biochemical functions, DNA binding and iron deposition, which complicates mechanistic studies of its contribution to stress survival. We have dissected this complexity by selectively modifying specific Dps functions and assessing their individual contributions to stress protection. This approach has provided unprecedented insight into the mechanisms governing stress mediation by Dps, revealing that both of its biochemical activities are required for full preservation of biological viability, as well as DNA integrity, under a broad array of different stress conditions.

Lysine-based DNA interaction creates nonspecific binding. Although much effort has been made to identify the DNA sequence motifs that bind to nucleoid-associated proteins, very few DNA-binding amino acid motifs have been identified within nucleoid-associated proteins (26, 27). Differing members of the Dps protein family have been proposed to utilize several different mechanisms for Dps-DNA interaction (28–32). In *E. coli*, *Lactococcus lactis*, and *Deinococcus radiodurans*, the flexible N-terminal extension of Dps has been shown to be required for binding to DNA (15, 33, 34), although the specific amino acid residues involved in DNA interaction have not previously been identified.

In this work, we have found that the spaced lysine residues in the extended *E. coli* Dps N-terminal region bind to DNA (Fig. 3B). The Dps lysines, predicted to be positively charged under physiological conditions (15), could potentially interact with DNA exclusively on its negatively charged phosphate backbone, bypassing the need for a specific DNA sequence motif (7, 10). DNA binding by Dps has been proposed to partially involve ion bridges with the negatively charged surface of Dps, based on observations that Dps-DNA interaction is exceedingly sensitive to the precise concentration of Mg^{2+} ions (15, 35). This mode of binding may be more prominent at pH values and Mg^{2+} concentrations lower than those used in this study.

While Dps species that have been shown to bind DNA via their N-terminal regions also contain positively charged amino acids in their N-terminal regions, sequence alignment does not reveal conserved sequence motifs or a common spacing of positively charged amino acids in the N-terminal region. Secondary structure prediction software (Quick2D) indicated that the three lysine residues in the N-terminal regions of *E. coli*, *L. lactis*, and *D. radiodurans* are most probably located in an alpha helix in the extended tail in each case and are predicted to be disordered. Alteration of the individual lysines to alanines in the *E. coli* Dps N-terminal region is not predicted to affect the alpha-helical structure or the disordered region. This result suggests that impaired DNA binding of these mutant proteins is caused not by a change in the flexibility or structure of the N-terminal region but only by a change in its electrostatic charge.

Conserved ferroxidase active-site residues can enhance or decrease activity. In comparison to Dps DNA-binding ability, which is not shared by all family members and is carried out by several different types of binding signatures (5), the ferroxidase center of Dps proteins is highly conserved. However, few studies

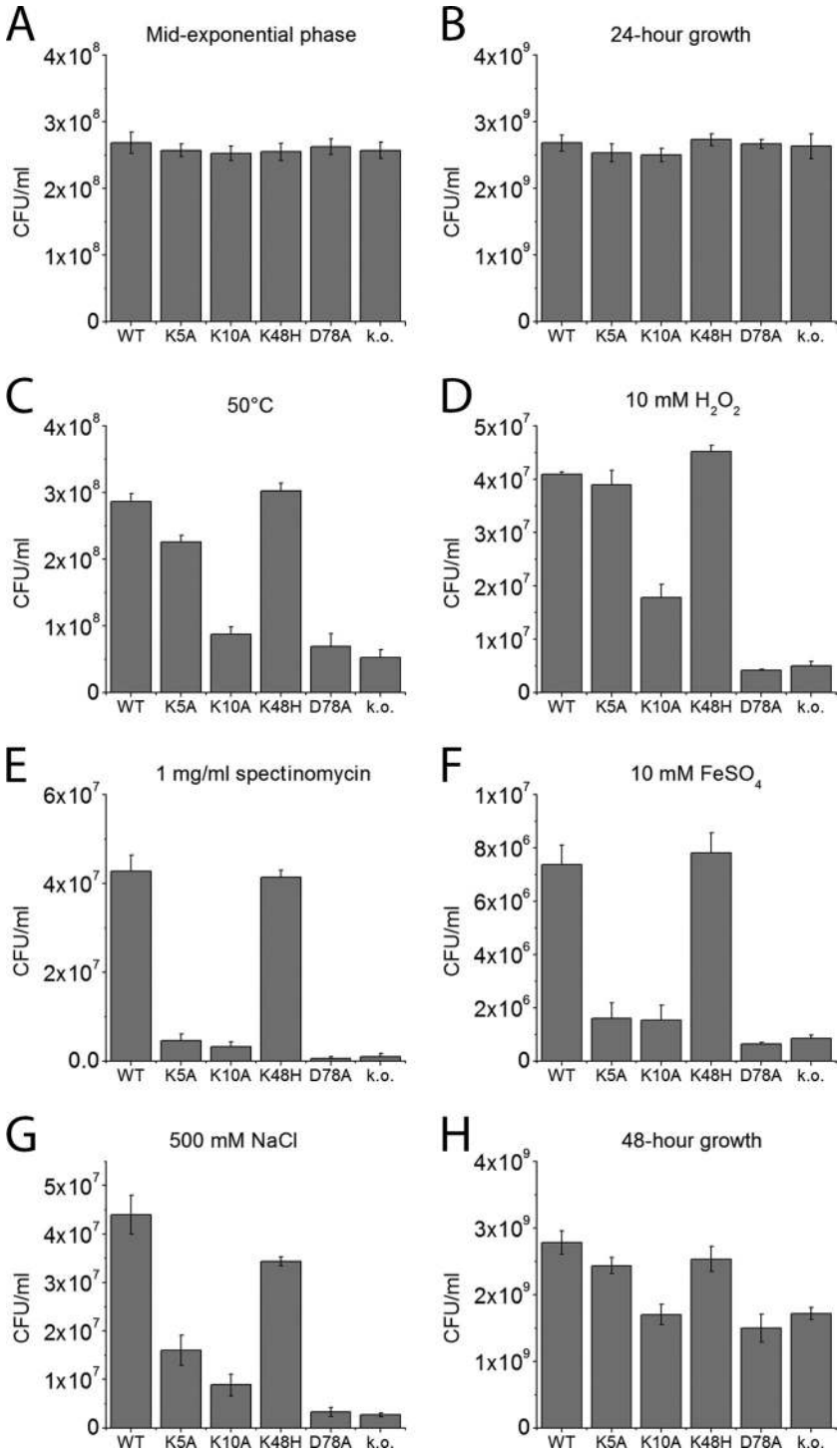

FIG 5 Preservation of cell viability from multiple stressors requires both activities of Dps. Shown are counts of CFU per milliliter of culture of *E. coli* strains with various *dps* sequences at mid-exponential-phase (A), after 24 h of growth (B), after exposure to heat shock (C), after exposure to hydrogen peroxide (D), after exposure to spectinomycin (E), after exposure to $FeSO_4$ (F), after exposure to osmotic stress (G), and after 48 h of growth (H). WT, wild type; k.o., knockout.

have attempted to determine the structure-function relationship between these conserved ferroxidase center residues and the resultant ferroxidase activity of Dps proteins. Asp78 has been shown to be one of the coordinating residues for strong iron binding site A, and our results indicate that it is indeed a vital contributor to Dps ferroxidase activity (Fig. 3A) (14). However, our experimental data show that the H51A mutation had no detectable effect on the iron oxidation rate (Fig. 3A). This result was unexpected since the Dps residue corresponding to His51 of *E. coli* Dps has been shown to be critical for the ferroxidase activity of *L. innocua* Dps (22) and

the presence of multiple histidines per ferroxidase center is an evolutionarily conserved feature (5). The failure of the H51A substitution to affect iron oxidation can perhaps be attributed to structural differences between the *L. innocua* and *E. coli* Dps proteins in the second metal coordination shell surrounding the ferroxidase center (5), leading to the H51A substitution creating differing conformational changes in the two homologs.

In order to create Dps with increased ferroxidase activity, we attempted to increase the affinity of the secondary iron-binding site in *E. coli* Dps. The weak B site is occupied by water under many conditions (14, 16) and thus cannot catalyze iron oxidation. Increasing the affinity of the secondary site should, in theory, lead to more efficient binding and subsequent oxidation of iron. We removed the predicted salt bridge between Asp78 and Lys48 by introducing an additional histidine residue. Iron oxidation by K48H mutant Dps was up to 100% higher than that by the wild type (Fig. 4B), verifying the hypothesis that Lys48 has an inhibitory effect on Dps ferroxidase activity.

Intriguingly, *E. coli* Dps has evidently not evolved to have maximally efficient iron oxidation properties, even though improvement of this ability would require only minor changes to its DNA sequence (Fig. 3B). While Dps does not play a major role in iron storage in *E. coli*, that job being largely carried out by ferritins and a bacterioferritin (36, 37), Dps ferroxidase activity is required for survival under many different stress conditions (Fig. 5). Unexpectedly, *E. coli* cells expressing K48H mutant Dps are not better protected against stressors than are cells expressing wild-type Dps (Fig. 5), suggesting that there may be little advantage in increased ferroxidase activity. Perhaps the inefficiency of *E. coli* Dps iron oxidation is compensated for by the massive upregulation of Dps expression that occurs in response to stresses such as starvation (7, 11), which would still allow for a robust enzymatic response to stressful conditions.

Each separable Dps activity provides direct protection of DNA. The biochemical DNA-binding and ferroxidase activity properties of our Dps variants revealed the finding that Dps activities are fully separable; specific engineered alterations of DNA binding affinity do not affect ferroxidase activity and vice versa. This feature has previously been hinted at by experiments showing that *L. innocua* Dps and *E. coli* Dps missing its first 18 amino acids, both of which exhibit poor DNA binding, can both still protect DNA from oxidative degradation (5, 15).

We aimed to test whether individual changes in Dps activity would have functional consequences for Dps protection. An *in vitro* DNA protection assay provided the result that each Dps DNA-binding mutant protein is weaker than wild-type Dps at preserving DNA (Fig. 4B). While a previous study did not observe a notable difference in DNA protection between wild-type Dps and a variant missing its first 18 amino acids that bound DNA poorly (15), our work tests a wider range of iron concentrations and reveals distinct deficiencies in protection by DNA-binding mutant proteins at higher iron concentrations. Among these Dps variants, even though DNA binding is important for *in vitro* DNA protection (Fig. 4), the affinity for DNA is not correlated with a protective effect (Fig. 2 and 4). Our results also indicate that the Lys5 residue has a function different from those of both Lys8 and Lys10. These lysines could potentially contribute unequally to two parallel and only partially dependent processes, DNA binding and DNA condensation (15), of which DNA condensation would be more crucial to DNA protection.

Contrary to DNA binding affinity, Dps ferroxidase activity shows an excellent correlation with the protective effect (Fig. 4C). Compared to wild-type Dps, the three ferroxidase center mutant proteins show better (K48H), equivalent (H51A), and worse (D78A) levels of DNA protection, exactly paralleling their relative abilities to oxidize iron. The difference between the best and worst performers in the group is dramatic, which suggests that ferroxidase activity is of key importance under these conditions. Overall, we can conclude that both DNA-binding and ferroxidase activities are involved in oxidative stress mediation by Dps *in vitro*.

Separable Dps activities work together to protect cells. To assess the individual contribution of each Dps activity to cell survival, *dps* variants with altered ferroxidase or DNA-binding activities were engineered into the chromosome of a wild-type *E. coli* strain, replacing the wild-type *dps* gene. The engineered strains were subjected to numerous types of stressors, which varied in both physical and chemical natures and which cause the induction of several differing *E. coli* stress mediation pathways (1, 38, 39). Previous studies of Dps have suggested that the different activities of Dps could contribute to the survival of different types of stress (7, 17, 24). However, our results show that both the Dps DNA-binding and ferroxidase activities are required for Dps to protect cells against each different stressor tested (Fig. 5), in agreement with our finding that both Dps activities are also required to prevent oxidative degradation of DNA *in vitro* (Fig. 4).

Our results indicate that many stressors may cause both oxidative/metal stress, which can be directly neutralized by Dps ferroxidase activity, and physical targeting of the chromosome, which could be counteracted by Dps binding to and shielding of the chromosome. In the cases of iron and H_2O_2 stresses (Fig. 5D and F), the stress-inducing chemicals can be directly neutralized by Dps ferroxidase activity (17) and will also spontaneously create reactive oxygen species that can directly damage cellular DNA. During heat shock (Fig. 5C), respiration and chemical reaction rates are higher (40) and superoxide dismutase is upregulated (41), causing the formation of H_2O_2 that could be combated by both Dps activities. Both osmotic shock (Fig. 5G) and starvation (Fig. 5H) result in the upregulation of a suite of oxidative stress response genes and regulons, including OxyR and SoxR (42, 43), perhaps indicating that these stressors may also boost reactive oxygen species levels.

Recent work has shown that certain representatives of the major classes of antibiotics, including aminoglycosides, seem to cause cell death via pathways that do not involve reactive oxygen species (44, 45). However, our results indicate that spectinomycin, an aminoglycoside antibiotic that inhibits elongation during protein synthesis and interferes with membrane integrity (46, 47), damages cells through mechanisms that can be counteracted via both ferroxidase activity and DNA binding (Fig. 4E). This antibiotic may therefore indeed generate intracellular reactive oxygen species, at least at the high concentrations used in this study. Complete understanding of the mechanisms whereby Dps activities protect cells will require direct probing of the effect of Dps on intracellular levels of ferrous iron and reactive oxygen species molecules during stress, as well as investigation into whether Dps activities can influence DNA breakage and modification *in vivo*.

ACKNOWLEDGMENTS

We are grateful to Wilfred Hagen, Peter Chien, Michela de Martino, Katy Wei, and Jurriaan Sieben for fruitful discussions. We thank Cees Dekker

for his kind gift of P1 phage lysate and Bertus Beaumont for generous access to plasmids.

This work was supported by the Netherlands Organization for Scientific Research (NWO/OCW) and the Department of Bionanoscience of the Delft University of Technology.

REFERENCES

1. **Battesti A, Majdalani N, Gottesman S.** 2011. The RpoS-mediated general stress response in Escherichia coli. Annu Rev Microbiol **65:**189–213. http://dx.doi.org/10.1146/annurev-micro-090110-102946.
2. **Higgins D, Dworkin J.** 2012. Recent progress in Bacillus subtilis sporulation. FEMS Microbiol Rev **36:**131–148. http://dx.doi.org/10.1111/j.1574-6976.2011.00310.x.
3. **Meyer AS, Baker TA.** 2011. Proteolysis in the Escherichia coli heat shock response: a player at many levels. Curr Opin Microbiol **14:**194–199. http://dx.doi.org/10.1016/j.mib.2011.02.001.
4. **Meyer AS, Grainger DC.** 2013. The Escherichia coli nucleoid in stationary phase. Adv Appl Microbiol **83:**69–86. http://dx.doi.org/10.1016/B978-0-12-407678-5.00002-7.
5. **Chiancone E, Ceci P.** 2010. The multifaceted capacity of Dps proteins to combat bacterial stress conditions: detoxification of iron and hydrogen peroxide and DNA binding. Biochim Biophys Acta **1800:**798–805. http://dx.doi.org/10.1016/j.bbagen.2010.01.013.
6. **Altuvia S, Almirón M, Huisman G, Kolter R, Storz G.** 1994. The dps promoter is activated by OxyR during growth and by IHF and sigma S in stationary phase. Mol Microbiol **13:**265–272. http://dx.doi.org/10.1111/j.1365-2958.1994.tb00421.x.
7. **Almirón M, Link AJ, Furlong D, Kolter R.** 1992. A novel DNA-binding protein with regulatory and protective roles in starved Escherichia coli. Genes Dev **6:**2646–2654. http://dx.doi.org/10.1101/gad.6.12b.2646.
8. **Nair S, Finkel SE.** 2004. Dps protects cells against multiple stresses during stationary phase. J Bacteriol **186:**4192–4198. http://dx.doi.org/10.1128/JB.186.13.4192-4198.2004.
9. **Calhoun LN, Kwon YM.** 2011. Structure, function and regulation of the DNA-binding protein Dps and its role in acid and oxidative stress resistance in Escherichia coli: a review. J Appl Microbiol **110:**375–386. http://dx.doi.org/10.1111/j.1365-2672.2010.04890.x.
10. **Azam TA, Ishihama A.** 1999. Twelve species of the nucleoid-associated protein from Escherichia coli. Sequence recognition specificity and DNA binding affinity. J Biol Chem **274:**33105–33113.
11. **Ali Azam T, Iwata A, Nishimura A, Ueda S, Ishihama A.** 1999. Growth phase-dependent variation in protein composition of the *Escherichia coli* nucleoid. J Bacteriol **181:**6361–6370.
12. **Frenkiel-Krispin D, Ben-Avraham I, Englander J, Shimoni E, Wolf SG, Minsky A.** 2004. Nucleoid restructuring in stationary-state bacteria. Mol Microbiol **51:**395–405. http://dx.doi.org/10.1046/j.1365-2958.2003.03855.x.
13. **Wolf SG, Frenkiel D, Arad T, Finkel SE, Kolter R, Minsky A.** 1999. DNA protection by stress-induced biocrystallization. Nature **400:**83–85. http://dx.doi.org/10.1038/21918.
14. **Grant RA, Filman DJ, Finkel SE, Kolter R, Hogle JM.** 1998. The crystal structure of Dps, a ferritin homolog that binds and protects DNA. Nat Struct Biol **5:**294–303. http://dx.doi.org/10.1038/nsb0498-294.
15. **Ceci P, Cellai S, Falvo E, Rivetti C, Rossi GL, Chiancone E.** 2004. DNA condensation and self-aggregation of Escherichia coli Dps are coupled phenomena related to the properties of the N-terminus. Nucleic Acids Res **32:**5935–5944. http://dx.doi.org/10.1093/nar/gkh915.
16. **Ilari A, Ceci P, Ferrari D, Rossi GL, Chiancone E.** 2002. Iron incorporation into Escherichia coli Dps gives rise to a ferritin-like microcrystalline core. J Biol Chem **277:**37619–37623. http://dx.doi.org/10.1074/jbc.M206186200.
17. **Zhao G, Ceci P, Ilari A, Giangiacomo L, Laue TM, Chiancone E, Chasteen ND.** 2002. Iron and hydrogen peroxide detoxification properties of DNA-binding protein from starved cells. A ferritin-like DNA-binding protein of Escherichia coli. J Biol Chem **277:**27689–27696.
18. **Karas VO, Westerlaken I, Meyer AS.** 2013. Application of an *in vitro* DNA protection assay to visualize stress mediation properties of the Dps protein. J Vis Exp **75:**50390.
19. **Datsenko KA, Wanner BL.** 2000. One-step inactivation of chromosomal genes in Escherichia coli K-12 using PCR products. Proc Natl Acad Sci U S A **97:**6640–6645. http://dx.doi.org/10.1073/pnas.120163297.
20. **Zhou QM, Fan DJ, Xie JB, Liu CP, Zhou JM.** 2010. A method for generating precise gene deletions and insertions in Escherichia coli. World J Microbiol Biotechnol **26:**1323–1329. http://dx.doi.org/10.1007/s11274-009-0305-y.
21. **Steiner M, Lazaroff N.** 1974. Direct method for continuous determination of iron oxidation by autotrophic bacteria. Appl Microbiol **28:**872–880.
22. **Ilari A, Latella MC, Ceci P, Ribacchi F, Su M, Giangiacomo L, Stefanini S, Chasteen ND, Chiancone E.** 2005. The unusual intersubunit ferroxidase center of Listeria innocua Dps is required for hydrogen peroxide detoxification but not for iron uptake. A study with site-specific mutants. Biochemistry **44:**5579–5587.
23. **Grove A, Wilkinson SP.** 2005. Differential DNA binding and protection by dimeric and dodecameric forms of the ferritin homolog Dps from Deinococcus radiodurans. J Mol Biol **347:**495–508. http://dx.doi.org/10.1016/j.jmb.2005.01.055.
24. **Martinez A, Kolter R.** 1997. Protection of DNA during oxidative stress by the nonspecific DNA-binding protein Dps. J Bacteriol **179:**5188–5194.
25. **Toyokuni S, Sagripanti JL.** 1992. Iron-mediated DNA damage: sensitive detection of DNA strand breakage catalyzed by iron. J Inorg Biochem **47:**241–248. http://dx.doi.org/10.1016/0162-0134(92)84069-Y.
26. **Dillon SC, Dorman CJ.** 2010. Bacterial nucleoid-associated proteins, nucleoid structure and gene expression. Nat Rev Microbiol **8:**185–195. http://dx.doi.org/10.1038/nrmicro2261.
27. **Luijsterburg MS, White MF, van Driel R, Dame RT.** 2008. The major architects of chromatin: architectural proteins in bacteria, archaea and eukaryotes. Crit Rev Biochem Mol Biol **43:**393–418. http://dx.doi.org/10.1080/10409230802528488.
28. **Bozzi M, Mignogna G, Stefanini S, Barra D, Longhi C, Valenti P, Chiancone E.** 1997. A novel non-heme iron-binding ferritin related to the DNA-binding proteins of the Dps family in Listeria innocua. J Biol Chem **272:**3259–3265. http://dx.doi.org/10.1074/jbc.272.6.3259.
29. **Ceci P, Ilari A, Falvo E, Chiancone E.** 2003. The Dps protein of Agrobacterium tumefaciens does not bind to DNA but protects it toward oxidative cleavage: X-ray crystal structure, iron binding, and hydroxyl-radical scavenging properties. J Biol Chem **278:**20319–20326. http://dx.doi.org/10.1074/jbc.M302114200.
30. **Ceci P, Ilari A, Falvo E, Giangiacomo L, Chiancone E.** 2005. Reassessment of protein stability, DNA binding, and protection of Mycobacterium smegmatis Dps. J Biol Chem **280:**34776–34785. http://dx.doi.org/10.1074/jbc.M502343200.
31. **Ceci P, Mangiarotti L, Rivetti C, Chiancone E.** 2007. The neutrophil-activating Dps protein of Helicobacter pylori, HP-NAP, adopts a mechanism different from Escherichia coli Dps to bind and condense DNA. Nucleic Acids Res **35:**2247–2256. http://dx.doi.org/10.1093/nar/gkm077.
32. **Huergo LF, Rahman H, Ibrahimovic A, Day CJ, Korolik V.** 2013. *Campylobacter jejuni* Dps protein binds DNA in the presence of iron or hydrogen peroxide. J Bacteriol **195:**1970–1978. http://dx.doi.org/10.1128/JB.00059-13.
33. **Bhattacharyya G, Grove A.** 2007. The N-terminal extensions of Deinococcus radiodurans Dps-1 mediate DNA major groove interactions as well as assembly of the dodecamer. J Biol Chem **282:**11921–11930. http://dx.doi.org/10.1074/jbc.M611255200.
34. **Stillman TJ, Upadhyay M, Norte VA, Sedelnikova SE, Carradus M, Tzokov S, Bullough PA, Shearman CA, Gasson MJ, Williams CH, Artymiuk PJ, Green J.** 2005. The crystal structures of Lactococcus lactis MG1363 Dps proteins reveal the presence of an N-terminal helix that is required for DNA binding. Mol Microbiol **57:**1101–1112. http://dx.doi.org/10.1111/j.1365-2958.2005.04757.x.
35. **Frenkiel-Krispin D, Levin-Zaidman S, Shimoni E, Wolf SG, Wachtel EJ, Arad T, Finkel SE, Kolter R, Minsky A.** 2001. Regulated phase transitions of bacterial chromatin: a non-enzymatic pathway for generic DNA protection. EMBO J **20:**1184–1191. http://dx.doi.org/10.1093/emboj/20.5.1184.
36. **Abdul-Tehrani H, Hudson AJ, Chang YS, Timms AR, Hawkins C, Williams JM, Harrison PM, Guest JR, Andrews SC.** 1999. Ferritin mutants of *Escherichia coli* are iron deficient and growth impaired, and fur mutants are iron deficient. J Bacteriol **181:**1415–1428.
37. **Andrews SC.** 1998. Iron storage in bacteria. Adv Microb Physiol **40:**281–351. http://dx.doi.org/10.1016/S0065-2911(08)60134-4.
38. **Chiang SM, Schellhorn HE.** 2012. Regulators of oxidative stress response genes in Escherichia coli and their functional conservation in bacteria. Arch Biochem Biophys **525:**161–169. http://dx.doi.org/10.1016/j.abb.2012.02.007.
39. **Shimizu K.** 2013. Regulation systems of bacteria such as Escherichia coli in response to nutrient limitation and environmental stresses. Metabolites **4:**1–35. http://dx.doi.org/10.3390/metabo4010001.

40. **Hoffmann F, Weber J, Rinas U.** 2002. Metabolic adaptation of Escherichia coli during temperature-induced recombinant protein production: 1. Readjustment of metabolic enzyme synthesis. Biotechnol Bioeng **80:** 313–319.
41. **Privalle CT, Fridovich I.** 1987. Induction of superoxide dismutase in Escherichia coli by heat shock. Proc Natl Acad Sci U S A **84:**2723–2726. http://dx.doi.org/10.1073/pnas.84.9.2723.
42. **Gunasekera TS, Csonka LN, Paliy O.** 2008. Genome-wide transcriptional responses of *Escherichia coli* K-12 to continuous osmotic and heat stresses. J Bacteriol **190:**3712–3720. http://dx.doi.org/10.1128/JB.01990-07.
43. **Hengge-Aronis R.** 2002. Signal transduction and regulatory mechanisms involved in control of the sigma(S) (RpoS) subunit of RNA polymerase. Microbiol Mol Biol Rev **66:**373–395. http://dx.doi.org/10.1128/MMBR.66.3.373-395.2002.
44. **Keren I, Wu Y, Inocencio J, Mulcahy LR, Lewis K.** 2013. Killing by bactericidal antibiotics does not depend on reactive oxygen species. Science **339:**1213–1216. http://dx.doi.org/10.1126/science.1232688.
45. **Liu Y, Imlay JA.** 2013. Cell death from antibiotics without the involvement of reactive oxygen species. Science **339:**1210–1213. http://dx.doi.org/10.1126/science.1232751.
46. **Borovinskaya MA, Shoji S, Holton JM, Fredrick K, Cate JH.** 2007. A steric block in translation caused by the antibiotic spectinomycin. ACS Chem Biol **2:**545–552. http://dx.doi.org/10.1021/cb700100n.
47. **Kohanski MA, Dwyer DJ, Wierzbowski J, Cottarel G, Collins JJ.** 2008. Mistranslation of membrane proteins and two-component system activation trigger antibiotic-mediated cell death. Cell **135:**679–690. http://dx.doi.org/10.1016/j.cell.2008.09.038.
48. **Ninnis RL, Spall SK, Talbo GH, Truscott KN, Dougan DA.** 2009. Modification of PATase by L/F-transferase generates a ClpS-dependent N-end rule substrate in Escherichia coli. EMBO J **28:**1732–1744. http://dx.doi.org/10.1038/emboj.2009.134.
49. **Schmidt R, Zahn R, Bukau B, Mogk A.** 2009. ClpS is the recognition component for Escherichia coli substrates of the N-end rule degradation pathway. Mol Microbiol **72:**506–517. http://dx.doi.org/10.1111/j.1365-2958.2009.06666.x.